

ORIGINAL ARTICLE

Matrix remodeling-associated protein 8 is a marker of a subset of cancer-associated fibroblasts in pancreatic cancer

Ryosuke Ichihara¹ | Yukihiro Shiraki¹ | Yasuyuki Mizutani^{1,2} |
Tadashi Iida^{1,2} | Yuki Miyai¹ | Nobutoshi Esaki¹ | Akira Kato¹ | Shinji Mii¹ |
Ryota Ando¹ | Masamichi Hayashi³ | Hideki Takami³ | Tsutomu Fujii⁴ |
Masahide Takahashi⁵ | Atsushi Enomoto¹ 

¹Department of Pathology, Nagoya University Graduate School of Medicine, Nagoya, Japan

²Department of Gastroenterology and Hepatology, Nagoya University Graduate School of Medicine, Nagoya, Japan

³Department of Gastroenterological Surgery, Nagoya University Graduate School of Medicine, Nagoya, Japan

⁴Department of Surgery and Science, Faculty of Medicine, Academic Assembly, University of Toyama, Toyama, Japan

⁵International Center for Cell and Gene Therapy, Fujita Health University, Toyoake, Japan

Correspondence

Atsushi Enomoto, Department of Pathology, Nagoya University Graduate School of Medicine, 65 Tsurumai-cho, Showa-ku, Nagoya 466-8550, Japan.
Email: enomoto@iar.nagoya-u.ac.jp

Funding information

Japan Agency for Medical Research and Development, Grant/Award Numbers: 20gm0810007h0105, 20gm1210009s0102; Japan Society for the Promotion of Science, Grant/Award Numbers: 18H02638, 20H03467

Abstract

Cancer-associated fibroblasts (CAFs), a compartment of the tumor microenvironment, were previously thought to be a uniform cell population that promotes cancer progression. However, recent studies have shown that CAFs are heterogeneous and that there are at least two types of CAFs, that is, cancer-promoting and -restraining CAFs. We previously identified Meflin as a candidate marker of cancer-restraining CAFs (rCAFs) in pancreatic ductal adenocarcinoma (PDAC). The precise nature of rCAFs, however, has remained elusive owing to a lack of understanding of their comprehensive gene signatures. Here, we screened genes whose expression correlated with Meflin in single-cell transcriptomic analyses of human cancers. Among the identified genes, we identified matrix remodeling-associated protein 8 (*MXRA8*), which encodes a type I transmembrane protein with unknown molecular function. Analysis of *MXRA8* expression in human PDAC samples showed that *MXRA8* was differentially co-expressed with other CAF markers. Moreover, in patients with PDAC or syngeneic tumors developed in *MXRA8*-knockout mice, *MXRA8* expression did not affect the roles of CAFs in cancer progression, and the biological importance of *MXRA8*⁺ CAFs is still unclear. Overall, we identified *MXRA8* as a new CAF marker; further studies are needed to determine the relevance of this marker.

KEYWORDS

cancer-associated fibroblasts, immunoglobulin superfamily containing leucine-rich repeat, matrix remodeling-associated protein 8, Meflin, pancreatic cancer, tumor microenvironment

Abbreviations: CAF, cancer-associated fibroblasts; CHIKV, Chikungunya virus; ECM, extracellular matrix; FAP, fibroblast activation protein; FSP1, fibroblast-specific protein 1; HPF, high-power field; H&E, hematoxylin and eosin; iCAF, inflammatory CAF; IHC, immunohistochemistry; ISH, in situ hybridization; ISLR, immunoglobulin superfamily containing leucine-rich repeat; Meflin, mesenchymal stromal cell- and fibroblast-expressing Linx paralogue; MSC, mesenchymal stem cell; *MXRA8*, matrix remodeling-associated protein 8; myCAF, myofibroblastic CAF; pCAF, cancer-promoting CAF; PDAC, pancreatic ductal adenocarcinoma; PDGFR, platelet-derived growth factor receptor; PSC, pancreatic stellate cell; rCAF, cancer-restraining CAF; KO, knockout; WT, wild-type; α -SMA, α -smooth muscle actin.

This is an open access article under the terms of the Creative Commons Attribution-NonCommercial License, which permits use, distribution and reproduction in any medium, provided the original work is properly cited and is not used for commercial purposes.

© 2022 The Authors. *Pathology International* published by Japanese Society of Pathology and John Wiley & Sons Australia, Ltd

INTRODUCTION

Cancer-associated fibroblasts (CAFs) are a major compartment of the tumor microenvironment in human cancers.^{1–8} They produce excessive amounts of insoluble extracellular matrix (ECM) and soluble factors, including cytokines, chemokines, and growth factors.^{1–8} CAF proliferation is widely found in almost all types of human cancers and is prevalent in treatment-resistant solid tumors showing fibroinflammatory stromal reactions, such as pancreatic ductal adenocarcinoma (PDAC), biliary duct adenocarcinoma, and poorly differentiated tumors of various origins.^{9–11} When observing tissue sections stained with hematoxylin and eosin (H&E), it is difficult to precisely distinguish CAFs from histiocytes and spindle-shaped macrophages based on their morphology. Therefore, many researchers have aimed to identify CAF-specific markers, regardless of their involvement in the functions of CAFs.^{4–8} The most frequently used marker for CAFs across various tumor types is α -smooth muscle actin (α -SMA).^{12–14} However, α -SMA is highly expressed in non-CAFs, such as myoepithelial cells, pericytes, and smooth muscle cells, which are abundant in contractile organs (e.g., the prostate, uterus, and intestine). Moreover, α -SMA is also highly expressed in smooth muscle cells, which constitute the tunica media of middle- and large-sized vessels. Other markers of CAFs include fibroblast activation protein (FAP), fibroblast-specific protein 1 (FSP1/S100A4), podoplanin, C-X-C chemokine ligand 12, and platelet-derived growth factor receptors (PDGFRs), all of which are differentially expressed in CAFs with different specificities.^{3–8}

Recent studies have revealed the heterogeneity and diversity of CAFs, the extents of which depend on the organ in which the tumor arises.^{3–8} In PDAC, the most prevalent classifications of CAFs are α -SMA⁺ myofibroblastic CAFs (myCAFs), inflammatory CAFs (iCAFs) defined by the expression of inflammatory cytokines, such as interleukin-6 and leukemia inhibitory factor, and antigen presenting CAFs (apCAFs), which express MHC class II and CD74.^{15–19} myCAFs and iCAFs promote PDAC progression through different mechanisms, making these CAFs attractive targets for the development of new therapeutics for PDAC.^{15–19} For other types of cancer, there are various classifications of CAFs, most of which are based on data from single-cell transcriptomic analyses.^{20–23} The differences in CAF heterogeneity among tumors seem to depend on the features of tumor cells, including gene mutations and expression profiles, reminiscent of the tumor immune microenvironment that is shaped by tumor cells.^{24,25}

Recently, we and others have proposed a simpler classification system for CAFs in which CAFs are divided into two subpopulations: cancer-promoting CAFs

(pCAFs) and cancer-restraining CAFs (rCAFs).^{4,6,14} The existence of rCAFs was originally conceptualized based on findings demonstrating that genetic depletion of CAFs or pharmacological intervention affecting CAF proliferation unexpectedly led to tumor progression in PDAC mouse models and human PDAC.^{26,27} However, no rCAF-specific markers had been identified in both mice and humans. We recently showed that Meflin, a glycosylphosphatidylinositol-anchored protein, is a marker of rCAFs in PDAC and colon cancer through analysis of mouse models and human tumor tissue samples.^{14,28–31} A lineage-tracing experiment using Meflin reporter mice showed that Meflin expression was downregulated in CAFs, whereas α -SMA expression was upregulated during cancer progression.²⁹ This suggests that Meflin⁺ rCAFs give rise to Meflin^{-/low} α -SMA⁺ pCAFs and that the tumor stroma is composed of a mixture of these different CAFs.^{14,29} Meflin was previously identified as a marker of mesenchymal stem cells (MSCs) or their early progenitors, which preferentially localize around vessels.^{27,32–34} Therefore, rCAFs may actually represent undifferentiated MSCs themselves or their early progenitors that proliferate in tumor stroma.¹⁴ Our previous data showed that transforming growth factor- β , hypoxia, and substrate stiffness are major factors that induced Meflin downregulation in rCAFs/MSCs to differentiate into α -SMA⁺ CAFs.^{14,28,32} However, Meflin⁺ CAFs have not yet been fully characterized.

Accordingly, in this study, we aimed to identify gene expression profiles of Meflin⁺ CAFs in human cancers through analysis of multiple datasets from single-cell transcriptomic analyses. This approach led to the identification of matrix remodeling-associated protein 8 (*MXRA8*) as a new marker of CAFs that overlap with Meflin⁺ CAFs.

MATERIALS AND METHODS

Human PDAC tissue samples

Human PDAC tissue samples were obtained from patients with PDAC who underwent surgical operation from 2010 to 2015. The histology of all PDAC cases was determined by the Pathology Department of Nagoya University Hospital before initiating this study.

Mxra8-knockout (KO) mice

Wild-type (WT) C57BL/6 and *Mxra8*-KO mice (C57BL/6Nj-Mxra8^{em1(IMPC)J}/Mmjax; MMRRC stock #46123), which were generated by the International Knockout Mouse Consortium (IKMC) using CRISPR/Cas9-mediated genome engineering, were purchased from the Jackson Laboratory. Genomic DNA extracted from

mouse tails was used for polymerase chain reaction-based genotyping. The sequences of the primers used were as follows: common forward (Fwd), 5'-GGGTAACATGGCAACAAACC-3'; WT reverse (Rvs), 5'-AACGCTGTAGGTATTTTCACC-3'; mutant Rvs, 5'-TTGGGCTAACAGCATTTCCT-3'.

Single-cell RNA sequence analysis, histology, cell culture, and animal experiments

Detailed protocols are described in the Supporting Information Materials.

Statistical analyses

Data are presented as mean \pm standard deviations of the means. The means of the two groups were compared using unpaired *t*-tests. We used two-way analysis of variance followed by Sidak's test for multiple comparisons, with $\alpha=0.05$. Spearman analysis was used to determine the correlations between the expression of *MXRA8* and other CAF markers. For survival analyses, Kaplan–Meier plots were drawn, and statistical differences were evaluated using log-rank Mantel–Cox tests. Statistical analyses were conducted using GraphPad Prism 9 (GraphPad Software Inc.). Results with *p* values of less than 0.05 were considered significant in all statistical analyses.

RESULTS

Identification of *MXRA8* as a novel candidate CAF marker in human cancers

First, we analyzed publicly available datasets from single-cell transcriptomic analyses of cells isolated from human PDAC (CRA001160), non-small cell lung cancer (GSE131907), colon cancer (GSE132465), and breast cancer (GSE161529).^{35–38} We extracted 198 genes whose expression was correlated with that of the immunoglobulin superfamily containing leucine-rich repeat (*ISLR*), which encodes human Meflin, at the single-cell level, with a Spearman's correlation coefficient (ρ) of more than 0.3 across the four datasets (Figure 1a). Gene Ontology (GO) enrichment analysis showed that the resulting 198 genes were enriched for terms related to the organization of collagen and the ECM and the skeletal system development (Figure S1A), consistent with the reported role of Meflin in collagen production in tissue repair and skeletal development.^{28,32} Given our focus on CAF markers expressed on the plasma membrane or cell surface, we further selected cell adhesion and surface proteins

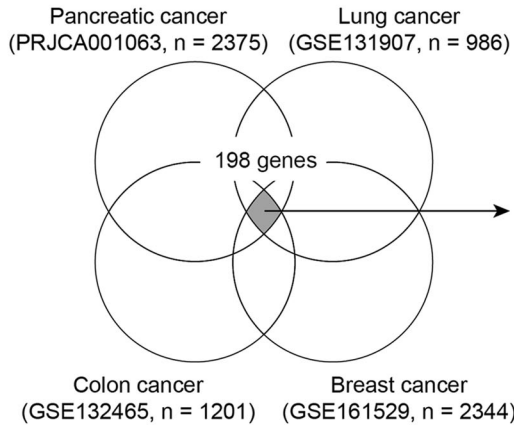
from the 198 genes but excluded extracellular space proteins and collagen-containing ECM proteins. The resulting genes were *MXRA8*, *CERCAM*, *THY1*, *BOC*, *SCARF2*, *DDR2*, *NLGN2*, *SSPN*, *PRPH2*, and *ADAM12* (Figure 1a). For subsequent analyses, we focused on *MXRA8*, which had the top score (0.660767). *MXRA8* encodes a type I transmembrane protein with 2 immunoglobulin-like domains whose function in cancer development and progression has not yet been addressed.³⁹

Clustering of cells included in the four datasets by UMAP plotting showed that *MXRA8* was specifically expressed in cell clusters that preferentially express the collagen type Ia1 (*COL1A1*) gene, a universal marker of fibroblasts (Figure 1b). Interestingly, *MXRA8* was also co-expressed with Meflin in all human cancers tested, suggesting the possibility that *MXRA8* may be a marker of CAFs in human cancers.

Mxra8 was expressed in distinct populations of fibroblasts in normal mouse tissues

We previously reported that Meflin is expressed by pancreatic stellate cells (PSCs) of the normal pancreas, which are one of the origins of CAFs in the pancreas.^{29,40,41} In situ hybridization (ISH) using an *Mxra8*-specific antisense probe on adult mouse tissues showed that *Mxra8* is expressed by rare stromal cells in the interstitium of the pancreas, the localization of which is similar to that of Meflin⁺ PSCs (Figure 2a).²⁹ An analysis of data from single-cell transcriptomic analysis (Tabula Muris)⁴² also confirmed that both *Mxra8* and Meflin (*Islr*) were expressed by PSCs in the adult mouse pancreas (Figure 2b). Furthermore, *Mxra8*⁺ cells were also found in the interstitium of the colon, lungs, and mammary glands, and these data were further corroborated by single-cell transcriptomic analysis (Figure 2c–e, S1B,C). These data suggest that *Mxra8* may be specifically expressed in fibroblasts in multiple mouse organs. Consistent with a previous study that Meflin⁺ fibroblasts comprise a subset of pericryptal fibroblasts,³⁰ *Mxra8* expression was detected in 58% \pm 14% and 32% \pm 8% of α -SMA (*Acta2*)- and Gremlin 1 (*Grem1*)-positive pericryptal fibroblasts, respectively (Figure S2A,B). In the lung, *Mxra8* expression was detected in 58% \pm 5% of cells that were positive for Transcription factor 21 (*Tcf21*), which is a known marker of lung lipofibroblasts⁴³ (Figure S2C). The expression of *MXRA8* in *TCF21*⁺ fibroblasts was also shown by an analysis of single-cell transcriptome data obtained from the lungs of healthy individuals⁴⁴ (Figure S2D). These data indicated that *Mxra8* is expressed in distinct subsets of fibroblasts in normal mouse tissues.

(a) Genes correlated with Meflin (*ISLR*) expression ($\rho > 0.3$)



- 1) Includes genes encoding cell adhesion proteins (GO: 0007155)
- 2) Excludes genes encoding extracellular space (GO: 0005615) and collagen-containing extracellular matrix proteins (GO: 0062023)

Gene name	Average Spearman's rank correlation coefficient
<i>MXRA8</i>	0.660767
<i>CERCAM</i>	0.651914
<i>THY1</i>	0.647224
<i>BOC</i>	0.644967
<i>SCARF2</i>	0.551734
<i>DDR2</i>	0.526610
<i>NLGN2</i>	0.516670
<i>SSPN</i>	0.457157
<i>PRPH2</i>	0.456980
<i>ADAM12</i>	0.453901

(b)

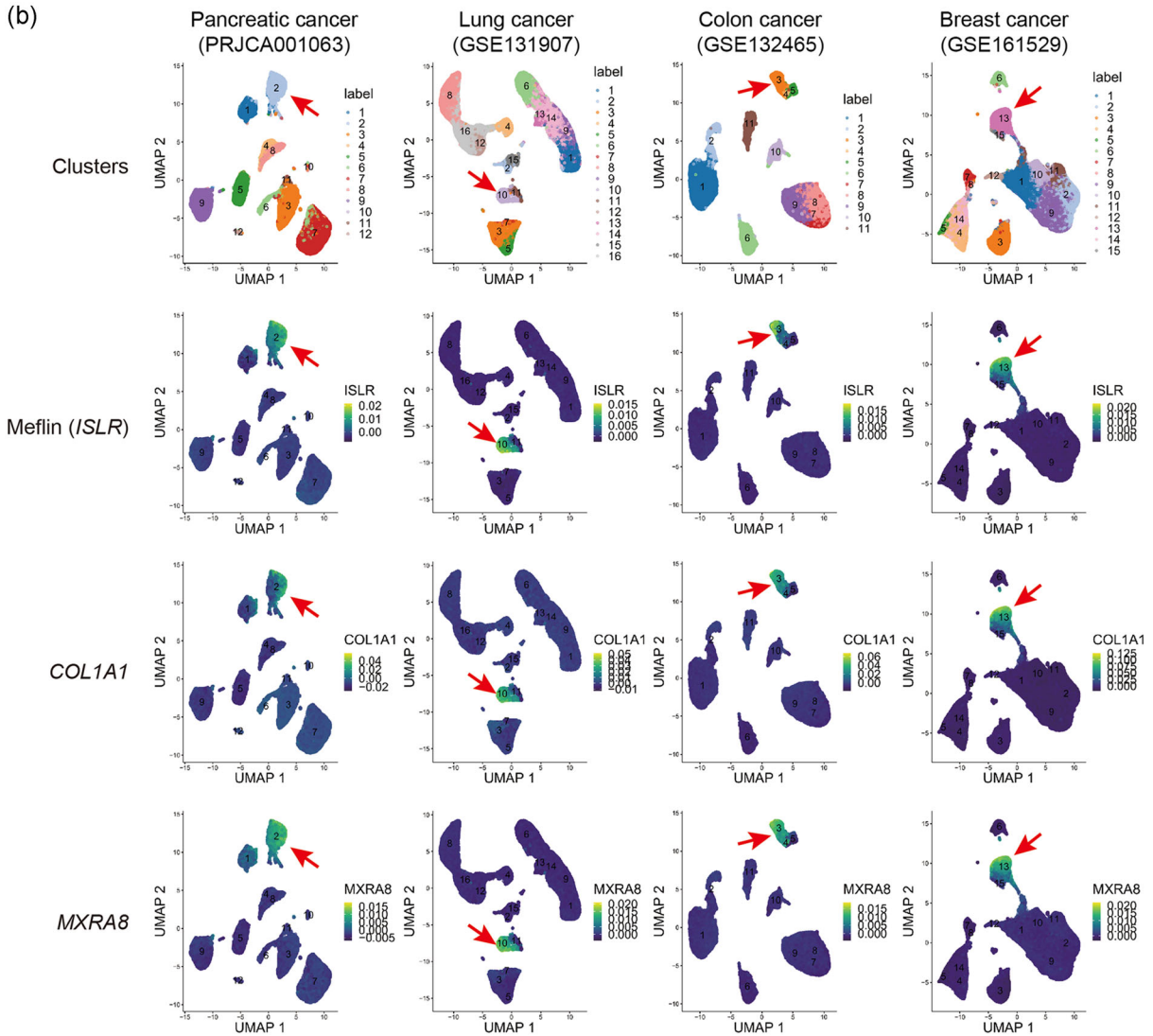


FIGURE 1 Identification of *MXRA8* as a candidate gene whose expression correlated with the expression of Meflin. (a) Datasets of single-cell transcriptomic analyses of cells isolated from human pancreatic ductal adenocarcinoma (PDAC) (CRA001160), non-small cell lung cancer (GSE131907), colon cancer (GSE132465), and breast cancer (GSE161529) were analyzed to extract 198 genes whose expression correlated with that of Meflin at the single-cell level, with Spearman's correlation coefficient (ρ) of more than 0.3 across the four datasets (left). Subsequently, genes encoding membrane or cell surface proteins were extracted based on Gene Ontology analysis (right). (b) UMAP plots showing distinct cell populations that were identified by single-cell RNA sequencing of all cells isolated from the four human cancers. The clusters indicated by arrows denote fibroblast clusters that exhibited high *COL1A1* expression. Note that both Meflin (*ISLR*) and *MXRA8* were specifically expressed in the fibroblast clusters

Localization of *MXRA8*⁺ cells in the normal human pancreas and PDAC

Next, we examined the localization of *MXRA8*⁺ cells in the normal human pancreas adjacent to PDAC by ISH (Figure 3a). *MXRA8*⁺ cells were found in the interstitium between acini or around the pancreatic ducts. *MXRA8* was not expressed by epithelial cells, such as acinar cells and duct cells, cells that constitute the islet of Langerhans, or endothelial cells, consistent with data from single-cell transcriptomic analysis (Figure 3a).

Notably, *MXRA8* expression was more evident in surgically resected human PDAC tissues (Figure 3b). ISH showed that *MXRA8* was expressed in stromal cells but not in other types of cells, including tumor and immune cells, in human PDAC. A combination of immunofluorescence and ISH also showed that *MXRA8* was not expressed by E-cadherin⁺ epithelial cells, including normal duct and tumor cells, CD3⁺ T cells, CD20⁺ B cells, or CD68⁺ macrophages (Figure 3c). These data suggested that *MXRA8* may be a marker of CAFs that proliferate in the stroma of human PDAC.

Inverse correlation between *MXRA8* and α -SMA (*ACTA2*) expression in CAFs from human PDAC

Because there are heterogenous populations of CAFs in human PDAC,^{16,18} we next examined the co-expression of *MXRA8* and other CAF markers (Figure 4a–d). Double staining for *MXRA8* by ISH and other CAF markers by immunohistochemistry (IHC) showed that *MXRA8* mRNA was detected in 30% \pm 15%, 46% \pm 17%, and 17% \pm 11% of α -SMA⁺, FAP⁺, and FSP1⁺ CAFs, respectively (Figure 4d). Double ISH showed that almost all (91% \pm 8.7%) Meflin (*ISLR*)-expressing cells were positive for *MXRA8*, whereas 56% \pm 15.2% of *MXRA8*-expressing cells were positive for Meflin, suggesting that these two genes may be co-expressed in the same CAFs, but *MXRA8* is expressed in a broader population of CAFs than Meflin in human PDAC (Figure 4e). Interestingly, quantification of ISH signals based on the number of dots per cell showed that *MXRA8* expression was weakly negatively correlated with *ACTA2*, which encodes α -SMA, and *PDGFRA*, but not Meflin (*ISLR*; Figure 4f). This was consistent with our previous study showing that Meflin expression was inversely correlated with α -SMA expression.²⁹ These data suggest that *MXRA8*⁺ cells may represent a CAF subpopulation distinct from conventional α -SMA⁺ myCAF⁺ but similar to Meflin⁺ rCAF⁺.

The inverse correlation between *MXRA8* and *ACTA2* expression was further supported by pseudotime analysis, in which we ordered all *COL1A1*⁺ fibroblasts of human PDAC along trajectories based on similarities in their gene expression patterns (Figure 5a–c). In this analysis, the *Pi16*⁺ fibroblast

subset was defined as a root for all fibroblasts to determine the direction of the trajectories, based on a recent report demonstrating that *Pi16* is a marker of universal fibroblasts giving rise to all types of fibroblasts under healthy and diseased conditions in mice.⁴⁵ The resulting trajectories were bifurcating, and one showed that Meflin (*ISLR*) and *MXRA8* were downregulated, whereas *ACTA2* was upregulated, over time (Figure 5b). The data supported the conversion of CAFs from Meflin (*ISLR*)⁺*MXRA8*⁺*ACTA2*^{low} to Meflin (*ISLR*)^{low}*MXRA8*^{low}*ACTA2*^{high} during PDAC progression, although further work is required to confirm these findings experimentally. Interestingly, we observed that small interfering RNA-mediated depletion of Meflin induced a decrease in *MXRA8* expression in a fibroblast cell line (Figure S3). The data suggested that *MXRA8* expression could be regulated downstream of Meflin, although the mechanism for this is unclear at present.

MXRA8 expression in CAFs was not correlated with outcomes in patients with PDAC

We previously showed that Meflin expression in CAFs was correlated with favorable outcomes in patients with PDAC.²⁹ Therefore, we next examined *MXRA8* expression in tissues surgically resected from 39 patients with PDAC using ISH analysis (Table S1). *MXRA8* ISH was considered positive if at least one dot within a CAF was stained positive (Figure 6a). We empirically divided the patients into *MXRA8*-high and -low groups based on the number of *MXRA8*⁺ CAFs per high-power field (HPF), followed by Kaplan–Meier analysis (Figure 6b,c). The data showed no significant correlation between the number of *MXRA8*⁺ CAFs and the overall survival rate in patients with PDAC. The significance of *MXRA8* expression in CAFs in the outcome of PDAC patients was also not demonstrated by an analysis of transcriptome data from a TCGA (The Cancer Genome Atlas) cohort (Figure 6d). Although not conclusive, these data suggested that the level of *MXRA8* determined by ISH may not be a good predictive marker of prognosis in patients with PDAC. In addition, *MXRA8* expression in CAFs seemed not to be affected by neoadjuvant chemotherapy, suggesting that *MXRA8*⁺ CAFs may not be targeted by cytotoxic anti-cancer drugs (Figure S4).

Mxra8 expression did not affect tumor growth in a heterotopic transplantation mouse model of pancreatic cancer

To further examine the roles of *Mxra8* in cancer progression, we adopted *Mxra8*-KO mice generated by The International Knockout Mouse Consortium using

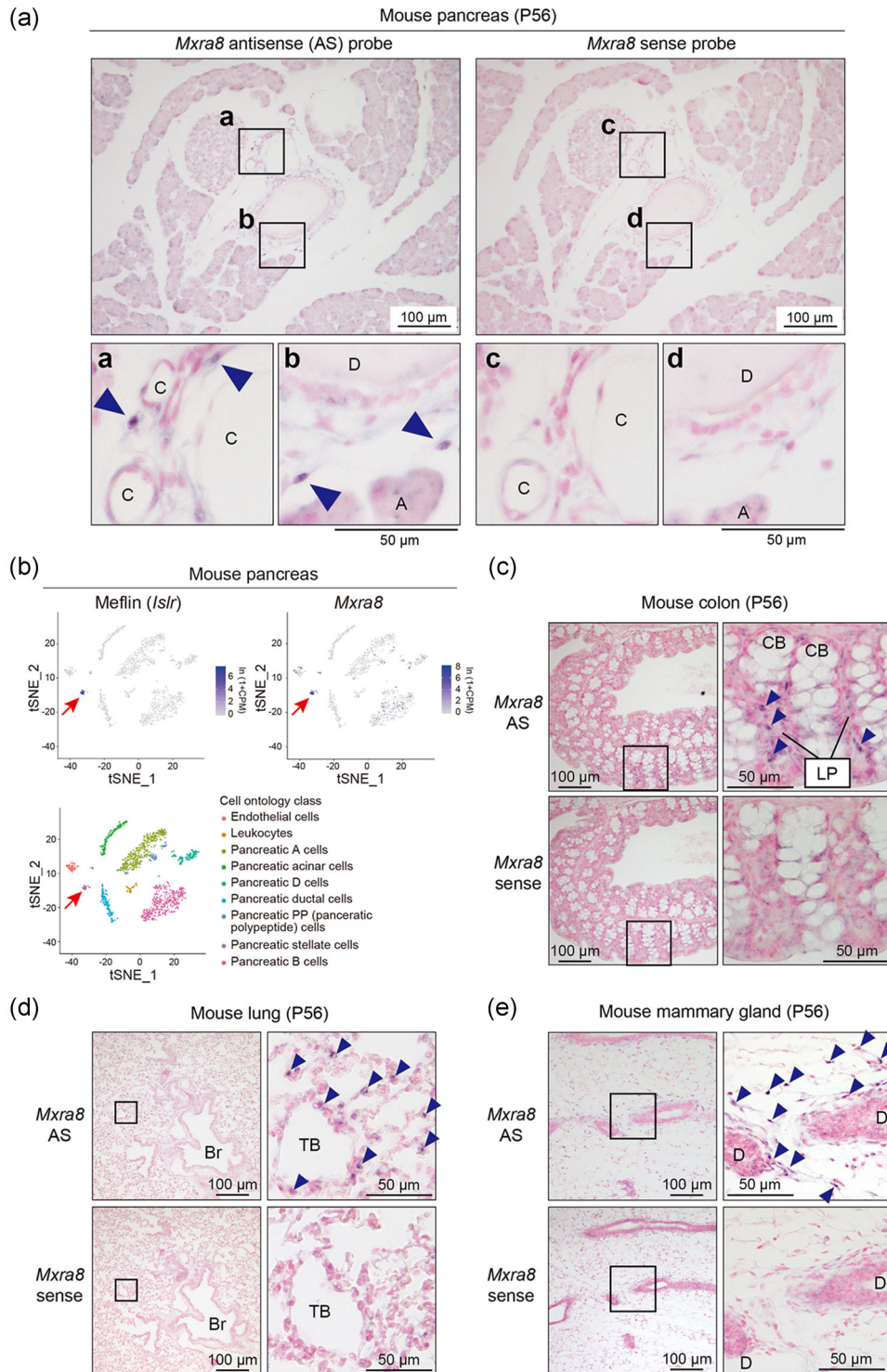


FIGURE 2 Expression patterns of *Mxra8* in mouse tissues. (a) In situ hybridization (ISH) with *Mxra8* antisense (AS, left) and control sense (right) probes was performed on pancreatic tissue sections from adult (P56) mice. Boxed regions (a–d) are magnified in lower panels. Arrowheads denote cells positive for *Mxra8*. C, capillaries; D, pancreatic duct; A, acini. (b) Analysis of *Mxra8* expression by single-cell RNA sequencing datasets (Tabula Muris, <https://tabula-muris.ds.czbiohub.org>) from mouse pancreatic cells. Distinct clusters corresponding to different cell populations in the adult mouse pancreas were identified and annotated post-hoc by Tabula Muris. Shown in the lower left panel is a t-distributed stochastic neighbor embedding (tSNE) plot showing 9 clusters of mouse pancreatic cells. Arrows indicate a cell population with a pancreatic stellate cell (PSC) signature. (c–e) ISH with *Mxra8* AS and control sense probes was performed on tissue sections from the mouse colon (c), lungs (d), and mammary glands (e) of adult (P56) mice. Boxed regions are magnified in adjacent panels. Arrowheads denote cells positive for *Mxra8*. CB, crypt base; LP, lamina propria; Br, bronchus; TB, terminal bronchiole; D, milk duct

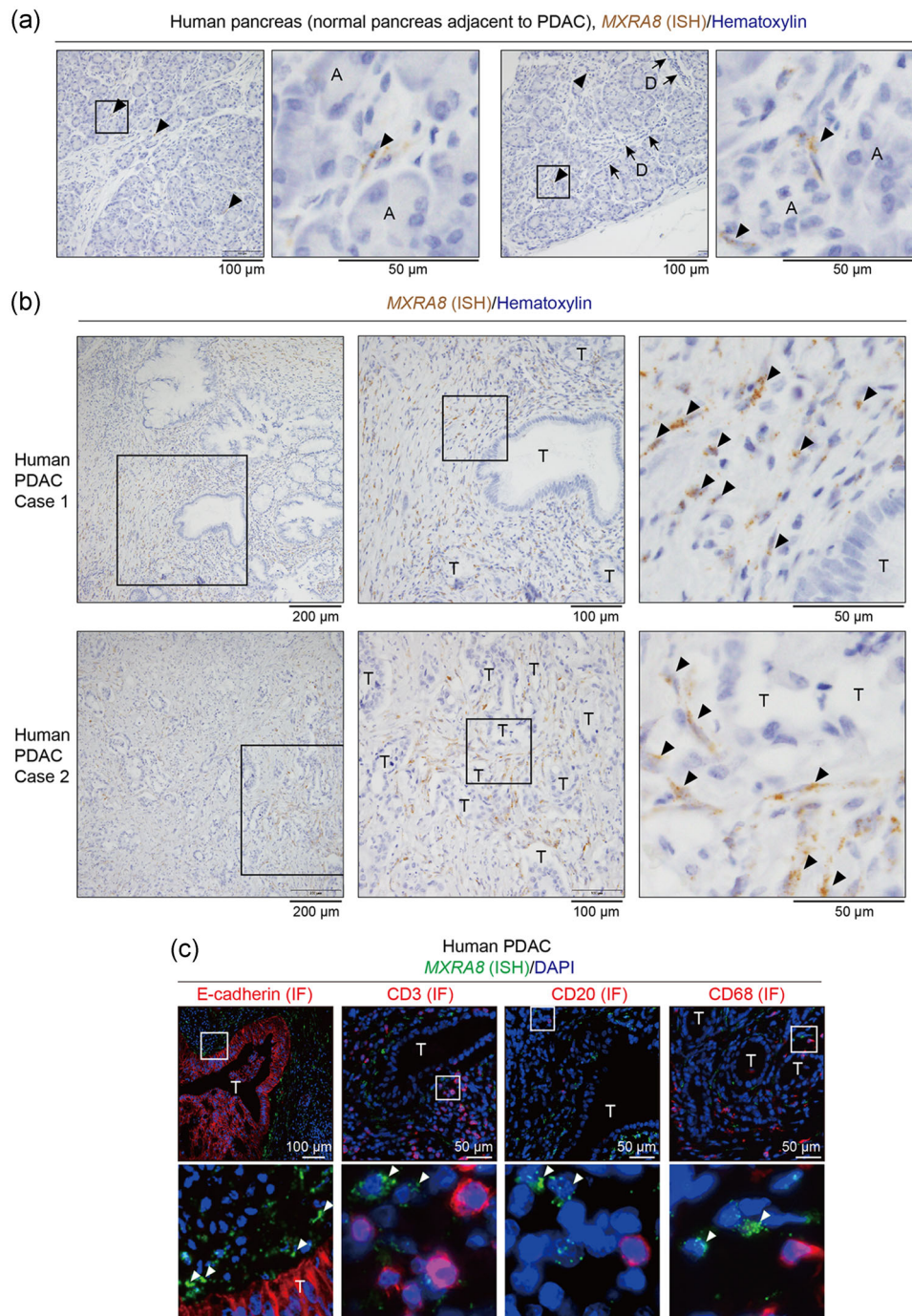


FIGURE 3 Expression pattern of *MXRA8* in normal human pancreatic tissues and pancreatic ductal adenocarcinoma (PDAC) tissues. (a) Expression of *MXRA8* in the human pancreas was examined by ISH. Boxed areas are magnified in adjacent panels. Arrowheads denote *MXRA8* signals found in stromal cells that represent PSCs. A, acini, D, pancreatic duct. (b) *MXRA8* expression in two representative cases of human PDAC. *MXRA8* expression was specifically found in stromal cells proliferating in the tumor stroma (arrowheads). T, tumor glands. (c) *MXRA8* was not expressed in tumor and immune cells in human PDAC. Tissue sections from a human PDAC tumor sample were stained for *MXRA8* by in situ hybridization (ISH) (green, arrowheads), followed by staining for E-cadherin, CD3, CD20, and CD68 by immunofluorescence. Boxed areas are magnified in lower panels. T, tumor glands

CRISPR/Cas9-mediated genome editing (Figure S5A,B). We found no apparent defects in growth rates or pancreatic histology in *Mxra8*-KO mice compared with WT littermates (Figure S5C–F). We subcutaneously transplanted syngeneic mouse pancreatic cancer cells

(mT5 cells)⁴⁶ into WT and *Mxra8*-KO male mice and then monitored the volumes and differentiation of the developed tumors (Figure S6A–D). The data showed that there were no significant differences between tumors developed in WT and *Mxra8*-KO mice. ISH then demonstrated

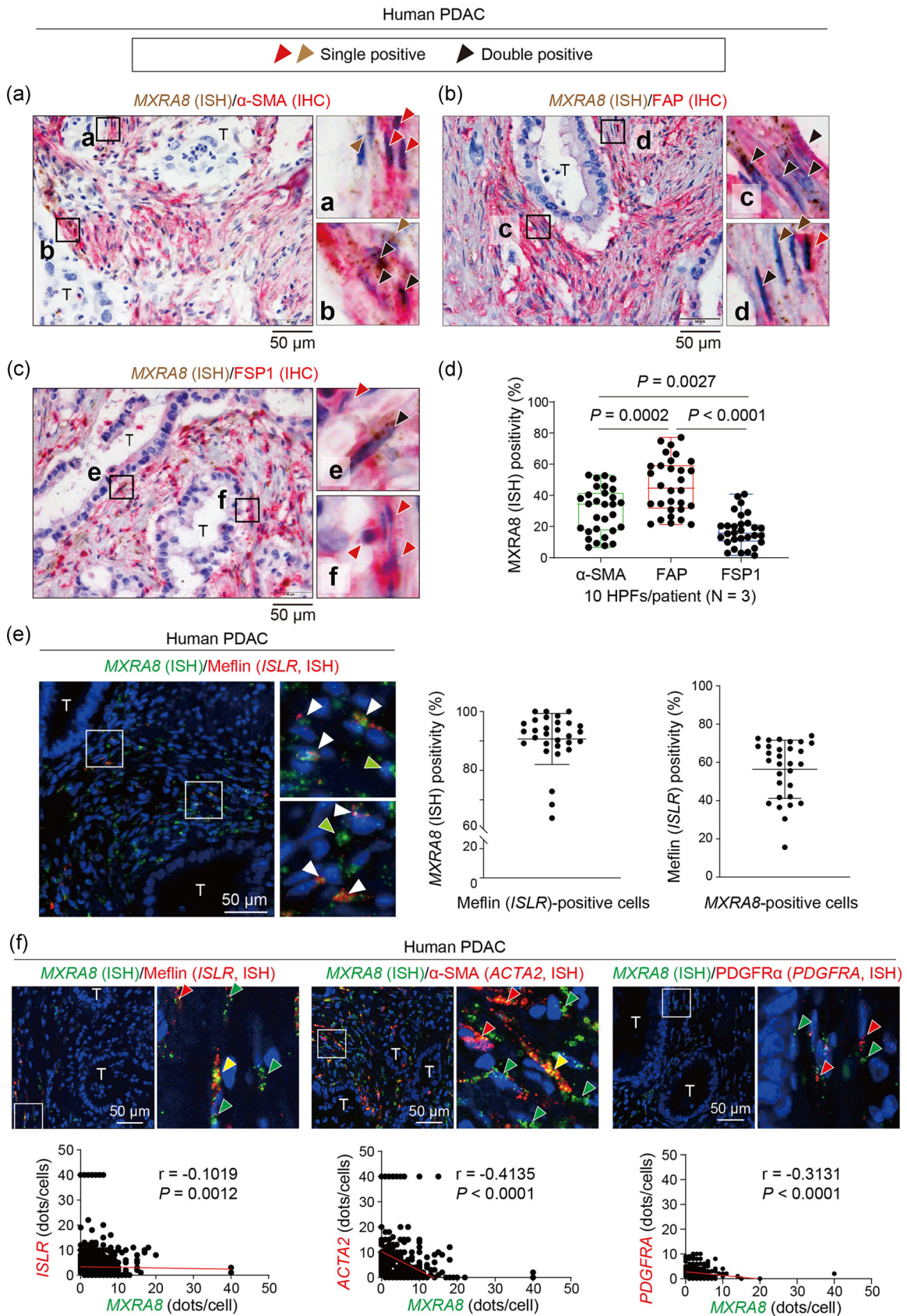


FIGURE 4 (See caption on next page)

that *Mxra8* was expressed in CAFs infiltrating in the stroma of the developed tumors in WT but not *Mxra8*-KO mice, suggesting that *Mxra8* may be a marker of CAFs in mice (Figure S6C).

We previously reported that tumors developed in Meflin-KO mice exhibited an increase in the number of Ki-67⁺ proliferating cells.²⁹ We therefore subjected tissue sections prepared from tumors developed in WT and *Mxra8*-KO mice to the same analyses. The data showed that the numbers of Ki-67⁺ proliferating cells and Meflin (*Islr*)⁺ CAFs were comparable between WT and *Mxra8*-KO tumors (Figure S6E,F). These data showed that loss of *Mxra8* expression in CAFs did not affect cancer cell proliferation or the infiltration of rCAF into the developed tumors.

***Mxra8* expression did not affect tumor differentiation in an orthotopic transplantation mouse model of pancreatic cancer**

We finally evaluated the roles of *Mxra8* in CAFs by orthotopically implanting mT5 mouse PDAC cells into the pancreases of WT and *Mxra8*-KO mice (Figure 7a). ISH showed *Mxra8* was expressed in CAFs in tumors developed in WT mice but not *Mxra8*-KO mice, confirming that *Mxra8* was a marker of CAFs (Figure 7b). Finally, H&E staining and IHC analysis showed that tumor differentiation and the numbers of Ki-67⁺ cells and Meflin (*Islr*)⁺ rCAF were comparable between WT and *Mxra8*-KO tumors (Figure 7c–e).

DISCUSSION

In the current study, we identified *MXRA8* as a novel marker of CAFs in both human and mouse PDAC by searching for genes that were co-expressed with Meflin. Similar to Meflin, *MXRA8* was found to be expressed in PSCs in the normal pancreas, which give

rise to CAFs in PDAC. Consistent with our recent hypothesis that Meflin⁺ CAFs represent rCAF in PDAC, the expression level of *MXRA8* was inversely correlated with that of *ACTA2*, a marker of conventional myCAF in PDAC. Thus, *MXRA8*⁺ CAFs may constitute a CAF subset distinct from α -SMA⁺ CAFs but comparable to Meflin⁺ rCAF. There were no commercially available antibodies that specifically detected *MXRA8* in IHC (data not shown); thus, we were not able to examine *MXRA8* expression at the protein level.

Our experiments on mouse tumor transplantation models, including orthotopic and subcutaneous transplantation, revealed no apparent effects of *MXRA8* expression in CAFs on PDAC progression. However, it would be premature to conclude that *MXRA8* is functionally neutral and not involved in the biological function of CAFs. A previous study showed that *MXRA8* physically interacts with $\alpha\beta$ 3 integrin, although the relevance of that interaction has not been clearly proven.⁴⁷ Given that $\alpha\beta$ 3 integrin is also expressed by PDAC and endothelial cells,⁴⁸ *MXRA8* expressed on CAFs may modulate the migration or proliferation of PDAC cells or tumor angiogenesis. Thus, the exact roles of *MXRA8* in PDAC progression and whether *MXRA8* is involved in the cancer-restraining function of rCAF should be determined by experiments on cultured fibroblasts and using more sophisticated PDAC mouse models, such as the KPC autochthonous model, in the future.^{29,49}

MXRA8 has attracted considerable attention in recent years because it was identified as a receptor for multiple arthritogenic alphaviruses, including Chikungunya virus (CHIKV), which is a globally emerging arthropod-transmitted virus.^{50,51} *MXRA8* binds directly to CHIKV particles, enhancing the attachment and internalization of the virus into cells.⁵⁰ One of the clinical symptoms of CHIKV infection is severe polyarthralgia lasting weeks to months.⁵² In our current study, we found that *MXRA8* was specifically expressed in fibroblasts in multiple organs, implying that fibroblasts in the joints, synovium, or

FIGURE 4 Differential co-expression of *MXRA8* with other cancer-associated fibroblast (CAF) markers in human pancreatic ductal adenocarcinoma (PDAC). (a)–(d) Expression of CAF markers in human PDAC was examined by alkaline phosphatase-based immunohistochemistry (IHC) for α -smooth muscle actin (α -SMA) (a), fibroblast activation protein (FAP) (b), and fibroblast-specific protein 1 (FSP1) (c) (red signals and red arrowheads) plus in situ hybridization (ISH) for *MXRA8* (brown signals and brown arrowheads). Black arrowheads denote cancer-associated fibroblasts (CAFs) expressing both *MXRA8* and α -SMA, FAP, or FSP1. Boxed regions were magnified in adjacent panels. In (d), *MXRA8* positivity in CAFs expressing α -SMA, FAP, or FSP1 was quantified by analyzing 10 high-power fields (HPFs) (400 \times) randomly selected from each patient ($N = 3$). T, tumor glands. (e) *MXRA8* (green) and Meflin (*ISLR*, red) expression in human PDAC was assayed by duplex ISH with custom RNAscope fluorescence probes, showing that the majority (90.7% \pm 8.7%) of Meflin (*ISLR*)⁺ CAFs were positive for *MXRA8* (white arrowheads), whereas 56.4% \pm 15.2% of *MXRA8*⁺ CAFs were positive for Meflin. Ten HPFs were randomly selected from each PDAC sample ($N = 3$) for histological evaluation. T, tumor gland. Green arrowheads, CAFs positive only for *MXRA8*. (f) Expression of *MXRA8* (green) and other CAF markers (red) was examined by duplex ISH. Boxed areas are magnified in adjacent panels. Note that some CAFs were double-positive for *MXRA8* and other CAF markers (yellow arrowheads), whereas the other CAFs were preferentially positive for either *MXRA8* (green arrowheads) or other CAF markers (red arrowheads). Lower panels show semiquantification of the expression of *MXRA8* and other CAF markers evaluated based on the number of dots per cell. All scoring was performed for randomly selected cells (*MXRA8*/*ISLR*, $N = 1002$; *MXRA8*/*ACTA2*, $N = 824$; *MXRA8*/*PDGFRA*, $N = 431$) in six HPFs from each human PDAC sample ($N = 2$). Spearman analysis was used to assess the correlations between the numbers of dots for each of the indicated genes. The red lines represent regression lines

(a) PRJCA001063 (Human PDAC) → *COL1A1*⁺ fibroblasts → Pseudotime analysis

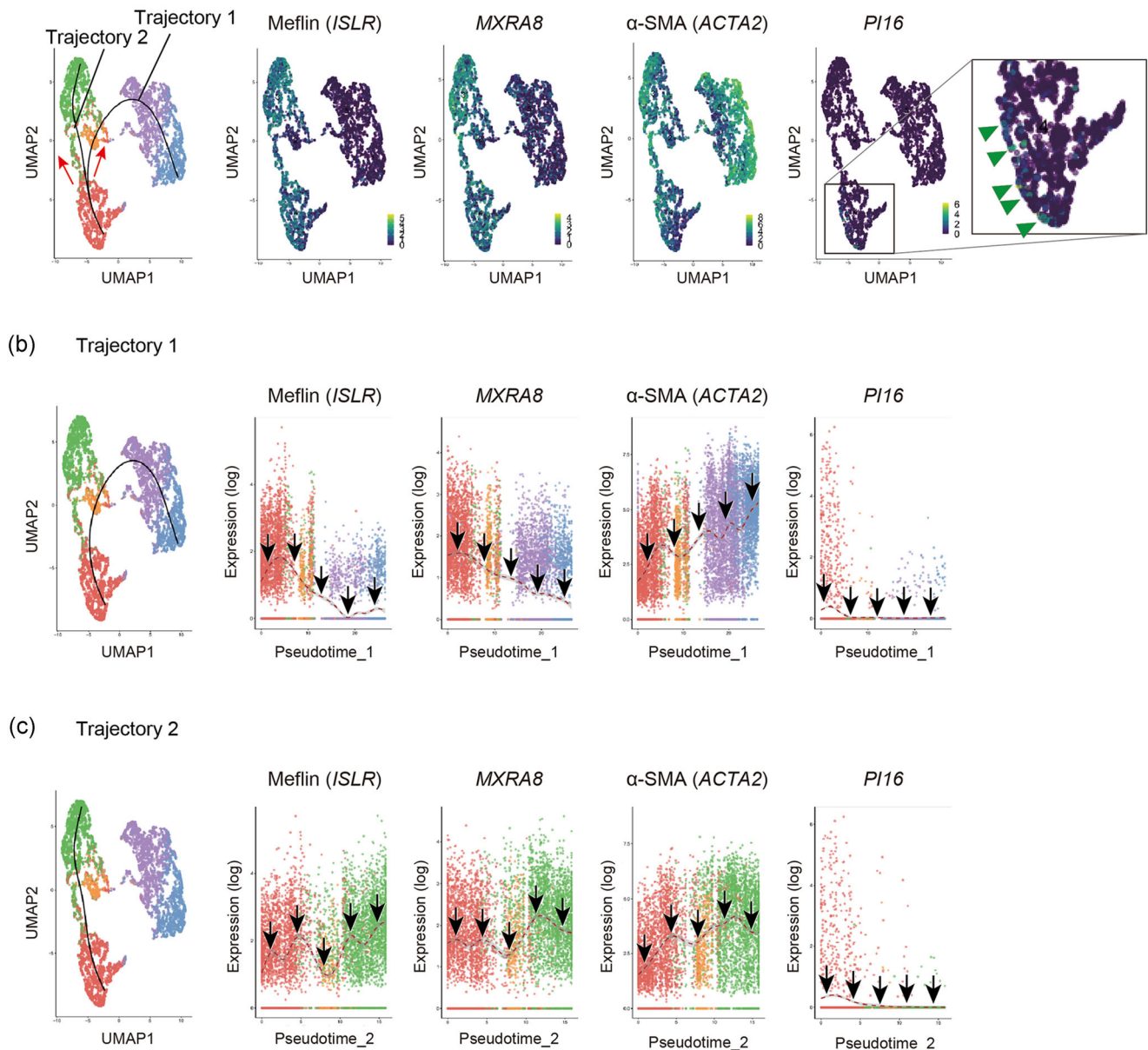


FIGURE 5 Pseudotime analysis of fibroblasts from human pancreatic ductal adenocarcinoma (PDAC) samples. (a) Single-cell pseudotime trajectories for fibroblasts in human PDAC tissues were computed using the algorithm slingshot with sequencing count data for single cells isolated from human PDAC (accession no. CRA001160). *COL1A1*⁺ cells were first extracted from all cells, followed by dimensionality reduction and clustering. The *PI16*⁺ cluster was set as the root of the trajectories, which led to the inference of two pseudotime trajectories (left panel). The other panels showed the expression of the indicated genes in the *COL1A1*⁺ cell clusters. (b), (c) Changes in the expression of the indicated genes in the two trajectories (b, trajectory 1; c, trajectory 2) inferred by the pseudotime analysis. Note that trajectory 1 showed the downregulation of *Meflin (ISLR)* and *MXRA8* and the upregulation of *ACTA2* over pseudotime (b)

muscles may be the primary sites of CHIKV infection. Notably, another study showed that *MXRA8* is also expressed in macrophages isolated from the bone marrow, which differed from our results demonstrating that *MXRA8* was not expressed by *CD68*⁺ macrophages infiltrating in the stroma of PDAC.⁵³ More detailed studies of the specific expression pattern of *MXRA8* will improve our understanding of the etiology and pathophysiology of CHIKV infection.

One interesting finding in the current study was the dynamic alteration of *MXRA8* expression in CAFs predicted from the pseudotime analysis. The data showed that *MXRA8* expression was downregulated following CAF activation, becoming positive for *ACTA2* during cancer progression. This finding further corroborated our hypothesis that *MXRA8* expression level was correlated with that of *Meflin*. A previous study using a *Meflin* reporter

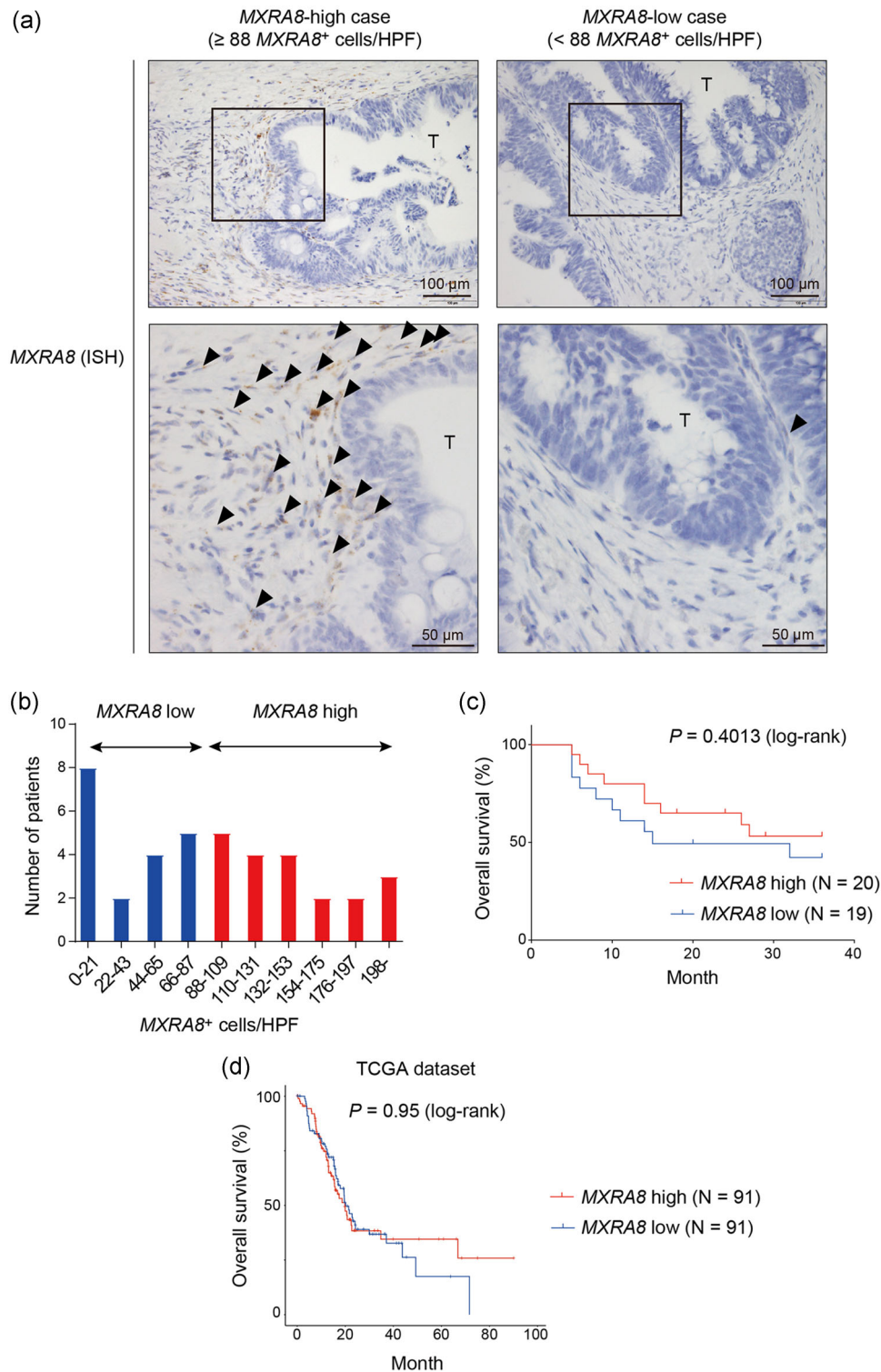


FIGURE 6 *MXRA8* expression was not correlated with outcomes in patients with pancreatic ductal adenocarcinoma (PDAC). (a) Representative in situ hybridization (ISH) images of *MXRA8*-high (left) and -low (right) cases. Arrowheads denote *MXRA8*⁺ CAFs. Boxed areas are magnified in adjacent panels. T, tumor glands. (b) Histogram of the distribution of patients with PDAC based on the mean numbers of *MXRA8*⁺ cells/high-power field (HPF). Three HPFs randomly selected from each patient were analyzed. The median number of *MXRA8*⁺ cells/HPF was 88, and this criterion was used to stratify the patients into *MXRA8*-high and -low cases. (c) Overall survival rates of patients with PDAC postsurgery in the *MXRA8*-high (red, N = 20) and -low (blue, N = 19) groups. (d) Overall survival rates of patients with PDAC stratified based on the transcriptome data from a TCGA cohort

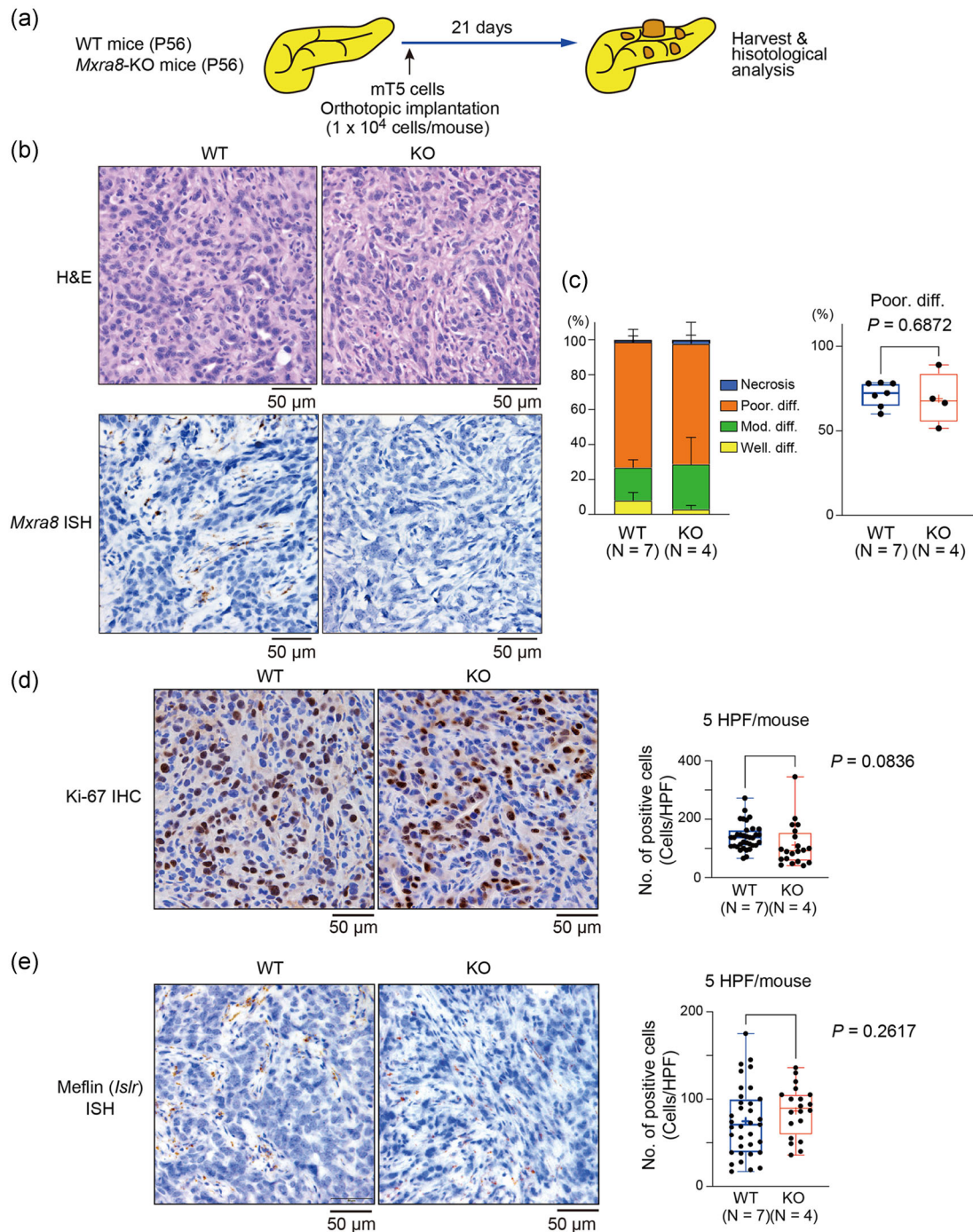


FIGURE 7 *Mxra8* expression in cancer-associated fibroblasts (CAFs) did not affect the progression of orthotopically transplanted pancreatic tumors in mice. (a) mT5 mouse pancreatic ductal adenocarcinoma (PDAC) cells (1×10^4 cells/mouse) were implanted into the pancreases of wild-type (WT) ($N = 7$) and *Mxra8*-knockout (KO) ($N = 4$) adult mice (P56), and histological analysis was performed 21 days after implantation. (b) Tissue sections obtained from tumors developed in WT and *Mxra8*-KO mice were stained for histology (H&E; upper) and *Mxra8* (ISH; lower). Note that the *Mxra8* mRNA signal (brown) was detected in cancer-associated fibroblasts (CAFs) from WT tumors but not *Mxra8*-KO tumors. (c) Histological evaluation of the differentiation types of tumors developed in the pancreases of WT and *Mxra8*-KO mice. Ten high-power fields (HPFs) were randomly selected from each tumor from WT ($N = 7$) and *Mxra8*-KO ($N = 4$) mice for histologic evaluation. The sum total area of each differentiation type was expressed relative to the area of the tumor (left). The percentages of the area of poorly differentiated type were not significantly different between WT and *Mxra8*-KO tumors. (d) Tissue sections obtained from tumors developed in WT (left, $N = 7$) and *Mxra8*-KO mice (right, $N = 4$) were stained for Ki-67 by immunohistochemistry (IHC), followed by quantification of the number of positive cells. Five HPFs obtained from each tumor were evaluated using ImageJ software. (e) Tissue sections obtained from tumors developed in WT (left, $N = 7$) and *Mxra8*-KO mice (right, $N = 4$) were stained for Meflin (*Islr*) mRNA by ISH, followed by quantification of the number of positive cells. Five HPFs obtained from each tumor were evaluated using ImageJ software

mouse line showed that Meflin expression in CAFs in the stroma of early-stage PDAC was significantly decreased, whereas *Acta2* expression was upregulated during cancer progression.^{14,29} This phenotypic conversion of CAFs (i.e., the CAF switch) may contribute to increased clinical malignancy and drug resistance in recalcitrant cancers, such as PDAC. Indeed, we recently reported that pharmacological and genetic approaches to revert fully activated CAFs or pCAF (Meflin weakly positive or negative) to rCAF (Meflin positive) were effective for improving tumor sensitivity to chemotherapeutics in PDAC mouse models.⁵⁴ Thus, it may be interesting to clarify whether *MXRA8* expression also undergoes dynamic alterations following pharmacological and genetic interventions to modulate CAF function.

Finally, the roles of *MXRA8* in the development and progression of fibrotic diseases should also be evaluated in future investigations. Consistent with our analysis, a previous study showed that *MXRA8* is specifically expressed in lipofibroblasts, a subset of lung fibroblasts.⁵⁵ Lipofibroblasts are known to be crucial for the maintenance of a subpopulation of alveolar type 2 cells, which have a high capacity for self-renewal.⁵⁶ In lung fibrosis, lipofibroblasts give rise to myofibroblasts, which cause the deposition of extensive ECM in the interstitium.⁵⁷ Recently, we and others reported that Meflin⁺ fibroblasts proliferate upon acute tissue injury or inflammation in the heart, intestines, and lungs and that these fibroblasts are essential for tissue regeneration and exhibit antifibrotic effects in subsequent fibrotic responses.^{32,58–60} However, in the current study, we did not observe any histological abnormalities in *Mxra8*-KO mice, and the physiological function of *MXRA8* remains unknown. Therefore, in future studies, researchers should evaluate whether *MXRA8* protein and *MXRA8*⁺ fibroblasts are involved in the etiology of various human fibrotic diseases.

ACKNOWLEDGMENTS

We thank David Tuveson (Cold Spring Harbor Laboratory) and Chang-il Hwang (UC Davis College of Biological Sciences) for providing the mouse PDAC cell lines mT5 and Kozo Uchiyama (Nagoya University) for technical assistance. This work was supported by a Grant-in-Aid for Scientific Research (B) (Grant Nos. 18H02638 to Atsushi Enomoto and 20H03467 to Masahide Takahashi) commissioned by the Ministry of Education, Culture, Sports, Science and Technology of Japan; Nagoya University Hospital Funding for Clinical Research (to Atsushi Enomoto); AMED-CREST (Japan Agency for Medical Research and Development, Core Research for Evolutional Science and Technology; Grant Nos. 20gm0810007h0105 and 20gm1210009s0102 to Atsushi Enomoto).

CONFLICT OF INTEREST

None declared.

ETHICS STATEMENT

Animal Experiments

All animal protocols were reviewed and approved by the Animal Care and Use Committee of Nagoya University Graduate School of Medicine (Approval No. 31229).

Human Tissue Samples

Human PDAC samples were obtained at the time of surgery from patients who had provided written informed consent. This study was conducted following the principles of the Declaration of Helsinki for Human Research and was approved by the Ethics Committee of Nagoya University Graduate School of Medicine (Approval No. 2017-0127-3).

AUTHOR CONTRIBUTIONS

Ryosuke Ichiara designed and performed the experiments, analyzed the data, and wrote the manuscript. Yukihiro Shiraki performed the experiments and the analysis on single-cell transcriptomic data. Yasuyuki Mizutani, Tadashi Iida, Yuki Miyai, Nobutoshi Esaki, Shinji Mii, Akira Kato and Ryota Ando assisted with histological and biochemical analyses. Masamichi Hayashi, Hideki Takami, and Tsutomu Fujii provided the clinical samples and intellectual input. Masahide Takahashi provided intellectual input. Atsushi Enomoto directed the project and wrote the manuscript.

REFERENCES

1. Bhowmick NA, Neilson EG, Moses HL. Stromal fibroblasts in cancer initiation and progression. *Nature* 2004;432:332–7.
2. Hanahan D, Weinberg RA. Hallmarks of cancer: the next generation. *Cell* 2011;144:646–74.
3. Öhlund D, Elyada E, Tuveson D. Fibroblast heterogeneity in the cancer wound. *J Exp Med*. 2014;211:1503–23.
4. Kalluri R. The biology and function of fibroblasts in cancer. *Nat Rev Cancer*. 2016;16:582–98.
5. Ishii G, Ochiai A, Neri S. Phenotypic and functional heterogeneity of cancer-associated fibroblast within the tumor microenvironment. *Adv Drug Deliv Rev*. 2016;99:186–96.
6. Kobayashi H, Enomoto A, Woods SL, Burt AD, Takahashi M, Worthley DL. Cancer-associated fibroblasts in gastrointestinal cancer. *Nat Rev Gastroenterol Hepatol*. 2019;16:282–95.
7. Sahai E, Astsaturov I, Cukierman E, DeNardo DG, Egeblad M, Evans RM, et al. A framework for advancing our understanding of cancer-associated fibroblasts. *Nat Rev Cancer*. 2020;20:174–86.
8. Mezawa Y, Orimo A. Phenotypic heterogeneity, stability and plasticity in tumor-promoting carcinoma-associated fibroblasts. *FEBS J*. 2021. <https://doi.org/10.1111/febs.15851>
9. Rizvi S, Gores GJ. Pathogenesis, diagnosis, and management of cholangiocarcinoma. *Gastroenterology* 2013;145:1215–29.
10. Neeße A, Algül H, Tuveson DA, Gress TM. Stromal biology and therapy in pancreatic cancer: a changing paradigm. *Gut* 2015;64:1476–84.
11. Neeße A, Bauer CA, Öhlund D, Lauth M, Buchholz M, Michl P, et al. Stromal biology and therapy in pancreatic cancer: ready for clinical translation? *Gut* 2019;68:159–71.

12. Sinn M, Denkert C, Striefler JK, Pelzer U, Stieler JM, Bahra M, et al. α -Smooth muscle actin expression and desmoplastic stromal reaction in pancreatic cancer: results from the CONKO-001 study. *Br J Cancer*. 2014;111:1917–23.
13. Valach J, Fik Z, Strnad H, Chovanec M, Plzák J, Cada Z, et al. Smooth muscle actin-expressing stromal fibroblasts in head and neck squamous cell carcinoma: increased expression of galectin-1 and induction of poor prognosis factors. *Int J Cancer*. 2012;131:2499–2508.
14. Miyai Y, Esaki N, Takahashi M, Enomoto A. Cancer-associated fibroblasts that restrain cancer progression: Hypotheses and perspectives. *Cancer Sci*. 2020;111:1047–57.
15. Öhlund D, Handly-Santana A, Biffi G, Elyada E, Almeida AS, Ponz-Sarvise M, et al. Distinct populations of inflammatory fibroblasts and myofibroblasts in pancreatic cancer. *J Exp Med*. 2017;214:579–96.
16. Elyada E, Bolisetty M, Laise P, Flynn WF, Courtois ET, Burkhart RA, et al. Cross-species single-cell analysis of pancreatic ductal adenocarcinoma reveals antigen-presenting cancer-associated fibroblasts. *Cancer Discov*. 2019;9:1102–23.
17. Biffi G, Oni TE, Spielman B, Hao Y, Elyada E, Park Y, et al. IL1-induced JAK/STAT signaling is antagonized by TGF β to shape CAF heterogeneity in pancreatic ductal adenocarcinoma. *Cancer Discov*. 2019;9:282–301.
18. Dominguez CX, Müller S, Keerthivasan S, Koeppen H, Hung J, Gierke S, et al. Single-cell RNA sequencing reveals stromal evolution into LRRC15⁺ myofibroblasts as a determinant of patient response to cancer immunotherapy. *Cancer Discov*. 2020;10:232–53.
19. Pereira BA, Vennin C, Papanicolaou M, Chambers CR, Herrmann D, Morton JP, et al. CAF subpopulations: a new reservoir of stromal targets in pancreatic cancer. *Trends Cancer* 2019;5:724–41.
20. Bartoschek M, Oskolkov N, Bocci M, Lötvrot J, Larsson C, Sommarin M, et al. Spatially and functionally distinct subclasses of breast cancer-associated fibroblasts revealed by single cell RNA sequencing. *Nat Commun*. 2018;9:5150.
21. Li H, Courtois ET, Sengupta D, Tan Y, Chen KH, Goh J, et al. Reference component analysis of single-cell transcriptomes elucidates cellular heterogeneity in human colorectal tumors. *Nat Genet*. 2017;49:708–18.
22. Wu F, Fan J, He Y, Xiong A, Yu J, Li Y, et al. Single-cell profiling of tumor heterogeneity and the microenvironment in advanced non-small cell lung cancer. *Nat Commun*. 2021;12:2540.
23. Vickman RE, Broman MM, Lanman NA, Franco OE, Sudyanti P, Ni Y, et al. Heterogeneity of human prostate carcinoma-associated fibroblasts implicates a role for subpopulations in myeloid cell recruitment. *Prostate* 2020;80:173–85.
24. Li J, Byrne KT, Yan F, Yamazoe T, Chen Z, Baslan T, et al. Tumor cell-intrinsic factors underlie heterogeneity of immune cell infiltration and response to immunotherapy. *Immunity* 2018;49:178–93.
25. Kumagai S, Togashi Y, Sakai C, Kawazoe A, Kawazu M, Ueno T, et al. An oncogenic alteration creates a microenvironment that promotes tumor progression by conferring a metabolic advantage to regulatory T cells. *Immunity* 2020;53:187–203.
26. Özdemir BC, Pentcheva-Hoang T, Carstens JL, Zheng X, Wu CC, Simpson TR, et al. Depletion of carcinoma-associated fibroblasts and fibrosis induces immunosuppression and accelerates pancreas cancer with reduced survival. *Cancer Cell* 2014;25:719–34.
27. Rhim AD, Oberstein PE, Thomas DH, Mirek ET, Palermo CF, Sastra SA, et al. Stromal elements act to restrain, rather than support, pancreatic ductal adenocarcinoma. *Cancer Cell* 2014;25:735–47.
28. Maeda K, Enomoto A, Hara A, Asai N, Kobayashi T, Horinouchi A, et al. Identification of Meflin as a potential marker for mesenchymal stromal cells. *Sci Rep*. 2016;6:22288.
29. Mizutani Y, Kobayashi H, Iida T, Asai N, Masamune A, Hara A, et al. Meflin-positive cancer-associated fibroblasts inhibit pancreatic carcinogenesis. *Cancer Res*. 2019;79:5367–81.
30. Kobayashi H, Gieniec KA, Wright JA, Wang T, Asai N, Mizutani Y, et al. The balance of stromal BMP signaling mediated by GREM1 and ISLR drives colorectal carcinogenesis. *Gastroenterology* 2021;160:1224–39.
31. Ohara Y, Enomoto A, Tsuyuki Y, Sato K, Iida T, Kobayashi H, et al. Connective tissue growth factor produced by cancer-associated fibroblasts correlates with poor prognosis in epithelioid malignant pleural mesothelioma. *Oncol Rep*. 2020;44:838–48.
32. Hara A, Kobayashi H, Asai N, Saito S, Higuchi T, Kato K, et al. Roles of the mesenchymal stromal/stem cell marker Meflin in cardiac tissue repair and the development of diastolic dysfunction. *Circ Res*. 2019;125:414–30.
33. Hara A, Kato K, Ishihara T, Kobayashi H, Asai N, Mii S, et al. Meflin defines mesenchymal stem cells and/or their early progenitors with multilineage differentiation capacity. *Genes Cells*. 2021;26:495–512.
34. Kuwano T, Izumi H, Aslam MR, Igarashi Y, Bilal M, Nishimura A, et al. Generation and characterization of a Meflin-CreERT2 transgenic line for lineage tracing in white adipose tissue. *PLoS One* 2021;16:e0248267.
35. Peng J, Sun BF, Chen CY, Zhou JY, Chen YS, Chen H, et al. Single-cell RNA-seq highlights intra-tumoral heterogeneity and malignant progression in pancreatic ductal adenocarcinoma. *Cell Res*. 2019;29:725–38.
36. Kim N, Kim HK, Lee K, Hong Y, Cho JH, Choi JW, et al. Single-cell RNA sequencing demonstrates the molecular and cellular reprogramming of metastatic lung adenocarcinoma. *Nat Commun*. 2020;11:2285.
37. Lee HO, Hong Y, Etioglu HE, Cho YB, Pomella V, Van den Bosch B, et al. Lineage-dependent gene expression programs influence the immune landscape of colorectal cancer. *Nat Genet*. 2020;52:594–603.
38. Pal B, Chen Y, Vaillant F, Capaldo BD, Joyce R, Song X, et al. A single-cell RNA expression atlas of normal, preneoplastic and tumorigenic states in the human breast. *EMBO J*. 2021;40:e107333.
39. Yonezawa T, Ohtsuka A, Yoshitaka T, Hirano S, Nomoto H, Yamamoto K, et al. Limitrin, a novel immunoglobulin superfamily protein localized to glia limitans formed by astrocyte endfeet. *GLIA* 2003;44:190–204.
40. Apte MV, Wilson JS, Lugea A, Pandolfi SJ. A starring role for stellate cells in the pancreatic cancer microenvironment. *Gastroenterology* 2013;144:1210–9.
41. Sherman MH, Yu RT, Engle DD, Ding N, Atkins AR, Tiriach H, et al. Vitamin D receptor-mediated stromal reprogramming suppresses pancreatitis and enhances pancreatic cancer therapy. *Cell* 2014;159:80–93.
42. The Tabula Muris Consortium, Overall Coordination, Logistical Coordination, Organ Collection and Processing; Library Preparation and Sequencing; Computational Data Analysis, et al. Single-cell transcriptomics of 20 mouse organs creates a *Tabula Muris*. *Nature* 2018;562:367–72.
43. Park J, Ivey MJ, Deana Y, Riggsbee KL, Sørensen E, Schwabl V, et al. The Tcf21 lineage constitutes the lung lipofibroblast population. *Am J Physiol Lung Cell Mol Physiol*. 2019;316:L872–85.
44. Valenzi E, Bulik M, Tabib T, Morse C, Sembrat J, Trejo Bittar H, et al. Single-cell analysis reveals fibroblast heterogeneity and myofibroblasts in systemic sclerosis-associated interstitial lung disease. *Ann Rheum Dis*. 2019;78:1379–87.
45. Buechler MB, Pradhan RN, Krishnamurthy AT, Cox C, Calviello AK, Wang AW, et al. Cross-tissue organization of the fibroblast lineage. *Nature* 2021;593:575–579.

46. Boj SF, Hwang CI, Baker LA, Chio II, Engle DD, Corbo V, et al. Organoid models of human and mouse ductal pancreatic cancer. *Cell* 2015;160:324–38.
47. Jung YK, Jin JS, Jeong JH, Kim HN, Park NR, Choi JY. DICAM, a novel dual immunoglobulin domain containing cell adhesion molecule interacts with alphavbeta3 integrin. *J Cell Physiol* 2008;216:603–14.
48. Hosotani R, Kawaguchi M, Masui T, Koshiba T, Ida J, Fujimoto K, et al. Expression of integrin $\alpha V\beta 3$ in pancreatic carcinoma: relation to MMP-2 activation and lymph node metastasis. *Pancreas* 2002;25:e30–e35.
49. Hingorani SR, Wang L, Multani AS, Combs C, Deramandt TB, Hruban RH, et al. Trp53R172H and KrasG12D cooperate to promote chromosomal instability and widely metastatic pancreatic ductal adenocarcinoma in mice. *Cancer Cell* 2005;7:469–83.
50. Zhang R, Kim AS, Fox JM, Nair S, Basore K, Klimstra WB, et al. Mxra8 is a receptor for multiple arthritogenic alphaviruses. *Nature* 2018;557:570–4.
51. Song H, Zhao Z, Chai Y, Jin X, Li C, Yuan F, et al. Molecular basis of arthritogenic alphavirus receptor MXRA8 binding to Chikungunya virus envelope protein. *Cell* 2019;177:1714–24.
52. Silva LA, Dermody TS. Chikungunya virus: epidemiology, replication, disease mechanisms, and prospective intervention strategies. *J Clin Invest* 2017;127:737–49.
53. Jung YK, Han SW, Kim GW, Jeong JH, Kim HJ, Choi JY. DICAM inhibits osteoclast differentiation through attenuation of the integrin $\alpha V\beta 3$ pathway. *J Bone Miner Res* 2012;27:2024–34.
54. Iida T, Mizutani Y, Esaki N, Ponik SM, Burkel BM, Weng L, et al. Conversion of cancer-associated fibroblasts from pro- to antitumor improves the sensitivity of pancreatic cancer to chemotherapeutics. *bioRxiv-Cancer Biol*. <https://doi.org/10.1101/2021.06.29.450327>
55. Angelidis I, Simon LM, Fernandez IE, Strunz M, Mayr CH, Greiffo FR, et al. An atlas of the aging lung mapped by single cell transcriptomics and deep tissue proteomics. *Nat Commun* 2019;10:963.
56. Juul NH, Stockman CA, Desai TJ. Niche cells and signals that regulate lung alveolar stem cells in vivo. *Cold Spring Harb Perspect Biol* 2020;12:a035717.
57. El Agha E, Moiseenko A, Kheirollahi V, De Langhe S, Crnkovic S, Kwapiszewska G, et al. Two-way conversion between lipogenic and myogenic fibroblastic phenotypes marks the progression and resolution of lung fibrosis. *Cell Stem Cell* 2017;20:261–73.
58. Xu J, Tang Y, Sheng X, Tian Y, Deng M, Du S, et al. Secreted stromal protein ISLR promotes intestinal regeneration by suppressing epithelial Hippo signaling. *EMBO J* 2020;39:e103255.
59. Nakahara Y, Hashimoto N, Sakamoto K, Enomoto A, Adams TS, Yokoi T, et al. Fibroblasts positive for meflin have anti-fibrotic property in pulmonary fibrosis. *Eur Respir J* 2021. <https://doi.org/10.1183/13993003.03397-2020>
60. Takahashi M, Kobayashi H, Mizutani Y, Hara A, Iida T, Miyai Y, et al. Roles of the mesenchymal stromal/stem cell marker Meflin/Islr in cancer fibrosis. *Front Cell Dev Biol* 2021;9:749924.

SUPPORTING INFORMATION

Additional supporting information may be found in the online version of the article at the publisher's website.

How to cite this article: Ichihara R, Shiraki Y, Mizutani Y, Iida T, Miyai Y, Esaki N, et al. Matrix remodeling-associated protein 8 is a marker of a subset of cancer-associated fibroblasts in pancreatic cancer. *Pathology International*. 2022; 72:161–175. <https://doi.org/10.1111/pin.13198>